

# Reverse of non-small cell lung cancer drug resistance induced by cancer-associated fibroblasts via a paracrine pathway

Quanhui Zhang<sup>1</sup>  | Junping Yang<sup>2</sup> | Jie Bai<sup>3</sup> | Jianzhuang Ren<sup>1</sup>

<sup>1</sup>Department of Intervention, The First Affiliated Hospital of Zhengzhou University, Zhengzhou, China

<sup>2</sup>Department of Dermatology, The First Affiliated Hospital of Zhengzhou University, Zhengzhou, China

<sup>3</sup>Department of Radiology, The First Affiliated Hospital of Zhengzhou University, Zhengzhou, China

## Correspondence

Quanhui Zhang and Jianzhuang Ren, Department of Intervention, The First Affiliated Hospital of Zhengzhou University, Zhengzhou, China.  
Emails: 1990876397@qq.com; rjzrk@126.com

## Funding information

The Research and Development of Biocompatible Airway Stent, Grant/Award Number: No. 2015AA020301

The tumor microenvironment orchestrates the sustained growth, metastasis and recurrence of cancer. As an indispensable component of the tumor microenvironment, cancer-associated fibroblasts (CAF) are considered as an essential synthetic machine producing various tumor components, leading to cancer sustained stemness, drug resistance and tumor recurrence. Here, we developed a sustainable primary culture of lung cancer cells fed with lung cancer-associated fibroblasts, resulting in enrichment and acquisition of drug resistance in cancer cells. Moreover, IGF2/AKT/Sox2/ABCB1 signaling activation in cancer cells was observed in the presence of CAF, which induces upregulation of P-glycoprotein expression and the drug resistance of non-small cell lung cancer cells. Our results demonstrated that CAF cells constitute a mechanism for cancer drug resistance. Thus, traditional chemotherapy combined with insulin-like growth factor 2 (IGF2) signaling inhibitor may present an innovative therapeutic strategy for non-small cell lung cancer therapy.

## KEYWORDS

cancer-associated fibroblasts, drug resistance, insulin-like growth factor 2, non-small cell lung cancer, P-glycoprotein

## 1 | INTRODUCTION

Lung cancer is the most common malignancy and has a high death rate worldwide. Non-small cell lung cancer (NSCLC) accounts for 80%-85% of lung cancers.<sup>1</sup> The morbidity and mortality rates of NSCLC are relatively high in China, with the 5-year survival rate less than 20%,<sup>2</sup> which is often due to the drug resistance developed after treatment for 1 year.<sup>3,4</sup> Traditional anticancer strategies targeted cancer cells as a separate group, but tumor cells develop in a complex microenvironment, which is crucial for the development of drug resistance.<sup>5</sup> Hence, specifically targeting the tumor microenvironment and reversing drug resistance have been suggested in recent 10 years as new strategies for cancer therapy.

It is clear that the development of drug resistance does not depend solely on cancer cell autonomous defects and is controlled by various important factors, including upregulation of ATP-binding

cassette (ABC) transporter proteins, DNA damage repair, anti-apoptotic protein such as BCL-2 expression, and activation of prosurvival pathway induced by tumor microenvironments.<sup>5</sup> The tumor microenvironment has received recent attention as an important determinant of cancer cells drug resistance.<sup>6</sup> A dominant of tumor microenvironment is cancer-associated fibroblasts (CAF),<sup>7</sup> and many studies in recent 20 years have suggested that CAF play a prominent functional role for these cells in relation to cancer behavior.<sup>8</sup> Cancer-associated fibroblasts (CAF) are spindle-shaped mesenchymal cells with characteristics of smooth muscle cells and fibroblasts in tumor tissues.<sup>9</sup> They participate in tumor growth and metastasis in several ways, such as through secretion of various tumor growth factors<sup>10</sup> or matrix metalloproteinases (MMP),<sup>11</sup> remodeling of the tumor microenvironment, and the induction of epithelial-mesenchymal transition (EMT) progress.<sup>12</sup> Cancer-associated fibroblasts (CAF) also play an important role in enhancing cancer cell resistance to multiple

This is an open access article under the terms of the Creative Commons Attribution-NonCommercial License, which permits use, distribution and reproduction in any medium, provided the original work is properly cited and is not used for commercial purposes.

© 2018 The Authors. *Cancer Science* published by John Wiley & Sons Australia, Ltd on behalf of Japanese Cancer Association.

drugs in various tumors, including breast cancer and colorectal carcinoma.<sup>13</sup> However, the specific mechanism of drug resistance induced by CAF remains unclear and it is still a challenge to effectively overcome the resistance and achieve better patient outcomes.

In the present study, enriched CAF were observed in tumor tissues from drug-resistant NSCLC patients. This tumor microenvironment with abundant CAF was demonstrated to facilitate the multi-drug resistance in lung cancer. Furthermore, our studies revealed that NSCLC drug resistance was regulated in an insulin-like growth factor 2 (IGF2)/insulin-like growth factor receptor-1 (IGF-1R)/AKT/Sox2/P-GP pathway. The application of IGF-1R inhibitor could reverse the drug resistance and inhibit the growth induced by CAF. Based on our results, we found that CAF might cause NSCLC drug resistance development, and chemotherapy combined with IGF-1R inhibitor could be a potential strategy to treat NSCLC.

## 2 | MATERIALS AND METHODS

### 2.1 | Patient samples

Non-small cell lung cancer tumor samples were obtained sterilely after surgery at The First Affiliated Hospital of Zhengzhou University and were sent to the laboratory within 4 hours. All samples were reviewed by a pathologist according to the World Health Organization classification of tumors. We excluded the samples from small cell lung cancer patients. The samples were divided into chemo-resistant and chemo-sensitive groups according to the clinical response. Sample collection and processing were carried out in accordance with the Declaration of Helsinki. Ethical approval was obtained from the Committee of the First Affiliated Hospital of Zhengzhou University. All subjects gave written informed consent. The clinical details of the patients with NSCLC are listed in Figure S1A. The details of the patient in whom LCP1 cells were successfully separated: male, 67 years old, 20 years smoking history, diagnosed as having stage IV NSCLC, with resistance to the cisplatin and etoposide chemotherapy program.

### 2.2 | Primary culture of fibroblasts and tumor cells

We cultured fibroblast cells from NSCLC tumor tissues. Briefly, after washing the samples with RPMI-1640 medium and PBS, the tissues were cut into pieces as small as possible. Then tissues were removed to another dish with DMEM (HyClone, USA) containing ACCUMAX (SIGMA, USA) medium to digest at 37°C, 5% CO<sub>2</sub> incubator for 2 hours, followed by filtration (BD Biosciences, San Jose, CA, USA). After washing with PBS, cell precipitation was collected and seeded into 6-well plates in 2-mL RPMI-1640 medium supplemented with 10% FBS overnight at 37°C. The next day, the medium was replaced with fresh medium to remove the nonadherent cells and the remaining cells were collected. After 5-10 passages, we sorted the CD90-positive cells with BD FACSAria III (USA) to collect fibroblasts and cultured the cells for further study.<sup>14</sup>

We also obtained primary tumor cells from NSCLC tumor tissues. Briefly, primary tumor specimens were finely minced and then were treated with collagenase II/IV to digest for 2 hours at 37°C, 5% CO<sub>2</sub> incubator. After this, the suspension was filtered and the tumor cells were cultured in RPMI-1640 containing EGF (Fusheng Company, Shanghai, China) and 10% FBS (Thermo Fisher Scientific, MA, USA). The media was changed every 4-5 days until cells covered the bottom. Then we sorted the CD45RA negative cells to culture and named it as LCP1.

### 2.3 | Cell lines and reagents

A549 was purchased from the Cell Bank of Chinese Academy of Sciences (Shanghai, China). All cell lines were cultured in RPMI-1640 (Invitrogen) supplemented with 10% FBS (Gibco), penicillin (100 U/mL) and streptomycin (0.1 mg/mL). Cisplatin, etoposide, doxorubicin, vinorelbine ditartrate and verapamil were purchased from Meilun Company (Da Lian, China). The recombinant IGF2 protein was purchased from Jinan Company (Shanghai, China). MK-2206 and OSI-906 were purchased from MedChemExpress (NJ, USA).

### 2.4 | Flow cytometry

It has been reported that CD90 was a marker for CAF.<sup>15</sup> Therefore, to detect the percent of CAF in lung cancer tumor samples, anti-CD90 human antibody (APC, eBioscience, USA) was added to the cell suspension which was obtained from chemo-resistant and chemo-sensitive lung cancer patients' tissues. After incubating for 30 minutes at room temperature, samples were detected with a BD Accuri C6 (USA) the isotype was stained as a negative control.

For the doxorubicin uptake experiment,  $5 \times 10^4$  A549 cells pre-co-cultured with CAF, IGF2, OSI-906, verapamil or not were seeded into a 6-well plate, followed by the doxorubicin treatment (1 µg/mL). Then cells were harvested at different time points (1, 2, 4 and 8 hours) to detect the intracellular doxorubicin fluorescence intensity by flow cytometry (BD Accuri C6).<sup>16</sup>

### 2.5 | Viability tests

All the cell viability in this study was measured by MTT assay. Briefly,  $2 \times 10^4$  A549 or LCP1 cells pre-co-cultured with CAF, IGF2 (50 ng/mL), OSI-906, MK-2206, siSox2, verapamil (50 nmol/L) or not were seeded into a 96-well plate; 24 hours later, the cells were treated with cisplatin (400 nmol/L), etoposide (150 µmol/L) and vinorelbine ditartrate (800 nmol/L). At the appropriate time points, the media was replaced by PBS containing MTT (0.5 mg/mL; Sigma-Aldrich; Merck Millipore) at 37°C for 4 hours, followed by the replacement with 150 µL dimethyl sulfoxide and then was shaken for 10 minutes to dissolve the crystals. The cell survival rates were estimated by the MTT assay at 620 nm with a microplate reader (Tecan, Männedorf, Switzerland).

## 2.6 | Real-time PCR

Total RNA was isolated from cells using TRIZOL (Invitrogen) and cDNA was synthesized using a Transcriptor First Strand cDNA Synthesis Kit (Toyobo, Osaka, Japan). A total of 2  $\mu$ g cDNA was used as the template to perform the quantitative real-time PCR for the detection of the target genes (SYBR Green real-time PCR master mixes, ThermoFisher Scientific, USA). The GAPDH was used as the internal control and 3 independent experiments were performed for each sample. The relative expression was quantified by normalizing the target gene level to the GAPDH using the  $\Delta\Delta$ Ct method. The primer pairs used are listed in Table S1.

## 2.7 | Drug retention assay

For the drug retention assay,  $2 \times 10^4$  A549 cells pre-co-cultured with CAF, IGF2, OSI-906, verapamil or not were seeded on 6-well chamber slides per well and treated with doxorubicin (1  $\mu$ g/mL) for 8 hours. The cells were then fixed, permeabilized and stained with DAPI (Jingrong Company, Shanghai, China). Since the doxorubicin has the spontaneous fluorescence, the drug retention in nucleus was visualized using an FV1000 (Leica) laser scanning confocal microscope.

## 2.8 | Drug efflux assay

The amount of doxorubicin released from A549 cells pre-co-cultured with CAF, IGF2, OSI-906 or not was detected by HPLC. The supernatants were harvested at different time points (1, 3, 6 and 12 hours) in this culture system to perform the HPLC. The HPLC system consisted of a 1525 Binary HPLC Pump, a 717 Plus Autosampler and a 2475 Multi-Wavelength Fluorescence Detector (Waters Corporation, Milford, CT, USA). Chromatography was performed on a column (4.6250 mm<sup>2</sup>, particle size 5 mm). The effluents were monitored at an excitation wave length of 480 nm and an emission wave length of 560 nm at 35°C. Detection and integration of chromatographic peaks was performed using Empower 2 software (Waters Corporation).

## 2.9 | Immunofluorescence staining and immunohistochemistry

To examine the expression of Sox2 following CAF co-culturing, A549 cells pre-treated with or without CAF were fixed and permeabilized. Then the cells were labeled with rabbit anti-Sox2 mAb (Abcam) and amplified with FITC goat anti-rabbit antibodies followed by Alexa 488 goat anti-FITC antibodies (Abcam). Nuclei were labeled with DAPI. To ensure the specificity of IF staining, primary antibodies were substituted with isotype-matched non-specific IgG in the experiment. All immunofluorescent images were captured using an FV1000 (Leica) laser scanning confocal microscope.

To examine the expression of  $\alpha$ -SMA and IGF2 in tumor tissues, immunohistochemistry was performed in tumor tissues from chemo-

sensitive and chemo-resistance patients. The tumor tissues were kept in 4% PFA overnight, then processed, embedded in paraffin, and sectioned at 4  $\mu$ m. Then the sections were blocked with 5% BSA in PBS and incubated with  $\alpha$ -SMA (1:200, Abcam) or IGF2 (1:100, Abcam) at 4°C overnight, followed by signal amplification using an ABC HRP Kit (Thermo, USA) and counter-staining with hematoxylin, dehydration with series of graded ethanol, and cleaning with xylene. A microscope (Leica, German) was used to visualize the sections.

## 2.10 | Western blotting

Protein was extracted from A549 cells with CAF, IGF2, anti-IGF2, MK-2206, siSox2 treatment or not by RIPA Lysis Buffer (Beyotime, Shanghai, China) containing protease plus phosphatase inhibitor cocktail. Western blot was performed by loading 20  $\mu$ g of protein lysates. Gradient 10%-15% gels were used to separate the electrophoretic protein in mono-dimension (Bio-Rad, CA, USA), and were then transferred onto a PVDF membrane (Millipore, Bedford, USA) by using the Trans-Blot Turbo Transfer System (Bio-Rad). Blots were blocked in 5% BSA in TBST for 1 hour at room temperature, and then were incubated overnight with the primary antibody of phospho-AKT (Thr308) (D25E6) (Cell Signaling Technology), total AKT (pan) (C67E7) (Cell Signaling Technology), Sox2 (D6D9) (Cell Signaling Technology), anti-P glycoprotein (P-GP) (ab129450) (Abcam) and  $\beta$ -actin (8H10D10) (Cell Signaling Technology) at 4°C. After washing, blots were incubated for 1 hour with a suitable secondary antibody (Auragene, Changsha, China). Proteins were visualized by ECL Western Blotting Substrate (Thermo Pierce, Rockford, IL).  $\beta$ -actin antibody was used as a control (ab8226, Abcam, UK).

## 2.11 | RNA interference

Human siRNA against Sox2 (siRNA1:5'-AAGGAGCACCC-3' and siRNA2:5'-GGATTATAAA-3') and control siRNA were purchased from Shanghai GenePharma. The transfection reagent and the siRNA complex were added to the A549 cells and incubated for 36 hours, followed by 24-hour IGF2 treatment. The cells were collected for further study.

## 2.12 | Animal assay

Female nude mice (4-5 weeks) were purchased from the SLAC Laboratory Animal Center (Shanghai, China) and kept under specific pathogen-free conditions. Tumors were established by the subcutaneous injection of  $2 \times 10^6$  A549 cells into the mice. Mice were randomly divided into 4 groups (6 mice in each group). Mice were treated with PBS, cisplatin, etoposide, vinorelbine ditartrate or OSI-906 once daily for 2 weeks, during which time tumor volume grew to 5  $\times$  5 mm. Tumor volume was measured and calculated using the following equation:  $V = (\text{length} \times \text{width}^2)/2$ . For survival curves, the death date of mice was recorded. The animal studies were conducted in accordance with the Public Health Service Policy and

approved by the Animal Care and Use Committee of the First Affiliated Hospital of Zhengzhou University. All the animal experiments complied with the WHO guidelines for the humane use and care of animals.

### 2.13 | Statistical analysis

All data were presented as mean  $\pm$  SEM. Graph Pad Prism 6.0 was used for data analysis ( $P < .05$ ). Student *t*-test was used to analyze the difference between groups. Survival analysis was performed by Kaplan–Meier method and evaluated using the log-rank test.  $P < .05$  was considered significant.

## 3 | RESULTS

### 3.1 | Cancer-associated fibroblast result in the acquisition of chemo-resistance in non-small cell lung cancer

The tumor microenvironment comprises immune cells, capillaries, fibroblasts and extracellular matrix. As a heterogeneous population of the tumor microenvironment, CAF enhance tumorigenesis of cancer cells.<sup>12,17</sup> To investigate whether CAF are involved in the NSCLC cell resistance to chemotherapeutic drugs, we analyzed the proportion of fibroblasts in chemo-sensitive and chemo-resistant NSCLC patients' tumor tissues (Figure S1A). We found that the chemo-resistant patients have increased fibroblasts compared to chemo-sensitive patients (Figure 1A,B). Based on this point, we hypothesize that the accumulation of CAF in lung cancer tissues may confer the

resistance of cancer cells to chemotherapy drugs. This was supported by the MTT assay, showing that pre-co-culturing with CAF (Figure S1B) from either chemo-sensitive (CS) or chemo-resistant (CR) samples increased the cell viability in the A549 lung cancer cells with cisplatin, etoposide and vinorelbine ditartrate treatment compared with monoculture (Figure 1C). Furthermore, we tested the primary tumor cells which were isolated from clinical NSCLC lung cancer patients' tumor tissue (labeled as LCP1 in Figure S1B) and found that pre-co-culturing with CAF from either chemo-sensitive (CS) or chemo-resistant (CR) samples could elevate the cell viability in LCP1 cells with cisplatin, etoposide and vinorelbine diatrate treatment (Figure 1D). These results suggest that CAF may participated in the acquisition of chemotherapeutic drugs resistance in NSCLC.

### 3.2 | Cancer-associated fibroblasts induce the acquired chemo-resistance through the insulin-like growth factor 2/insulin-like growth factor receptor-1 paracrine pathway

Next, we questioned how the CAF induced the chemo-resistance in NSCLC. It has been reported that CAF could secrete cytokines or other proteins to communicate with the surrounding cells for cell growth, differentiation or migration.<sup>18–20</sup> Based on this concept, we added the conditioned medium from fibroblasts culturing with tumor cells to the A549 and LCP1 cells followed by chemotherapy drugs treatment, respectively. The MTT assay showed that the conditioned medium significantly increased the cell viability in A549 and LCP1 cells with cisplatin, etoposide and vinorelbine diatrate treatment (Figure 2A,B). This data suggests that the CAF may produce soluble

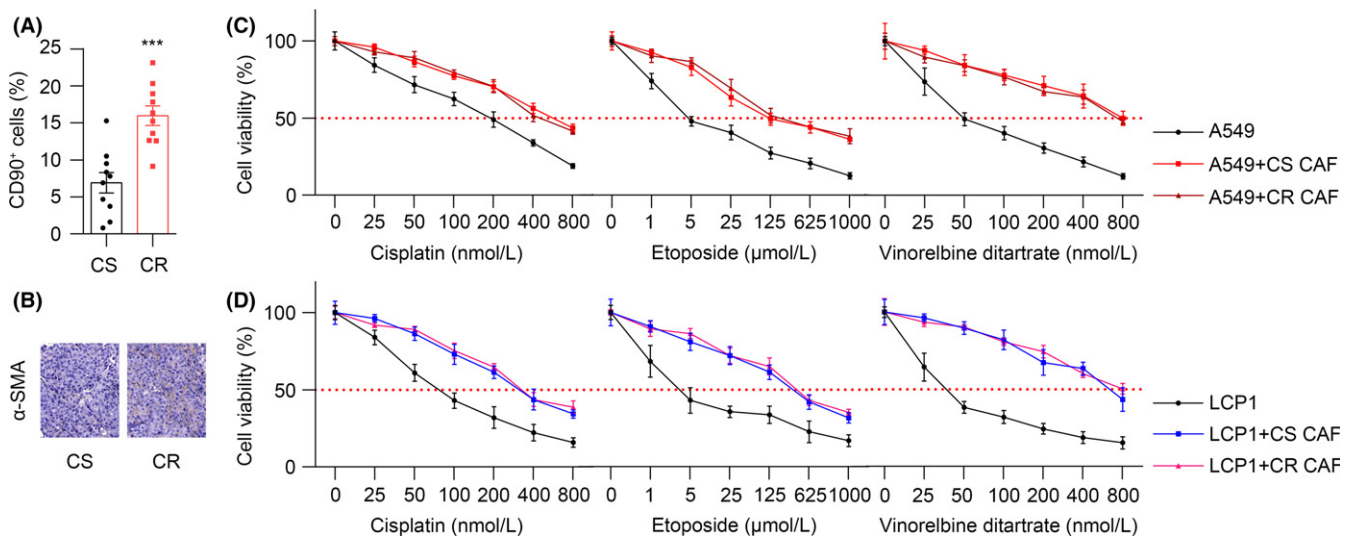


**FIGURE 1** Cancer-associated fibroblasts result in the acquisition of chemo-resistance in lung cancer. A, Quantification of the cancer-associated fibroblasts (CAF, CD90<sup>+</sup> cells) in chemo-sensitive (CS, n = 10) and chemo-resistant (CR, n = 10) lung cancer patients by flow cytometry. B,  $\alpha$ -SMA expression in CS and CR samples by immunohistochemistry staining. Scale bar is 50  $\mu$ m. C, MTT assay of A549 cells treated by different concentrations of cisplatin, etoposide and vinorelbine ditartrate, respectively, with or without CS or CR CAF pre-co-cultured (n = 3). D, The MTT assay of the primary lung cancer patient cells (LCP1) treated with different concentrations of cisplatin, etoposide and vinorelbine ditartrate, respectively, with or without CS or CR CAF pre-co-cultured (n = 3). The data are presented as the means  $\pm$  SEM from 3 independent experiments. \* $P < .05$ ; \*\* $P < .01$ ; \*\*\* $P < .001$ ; ns, not statistically significant

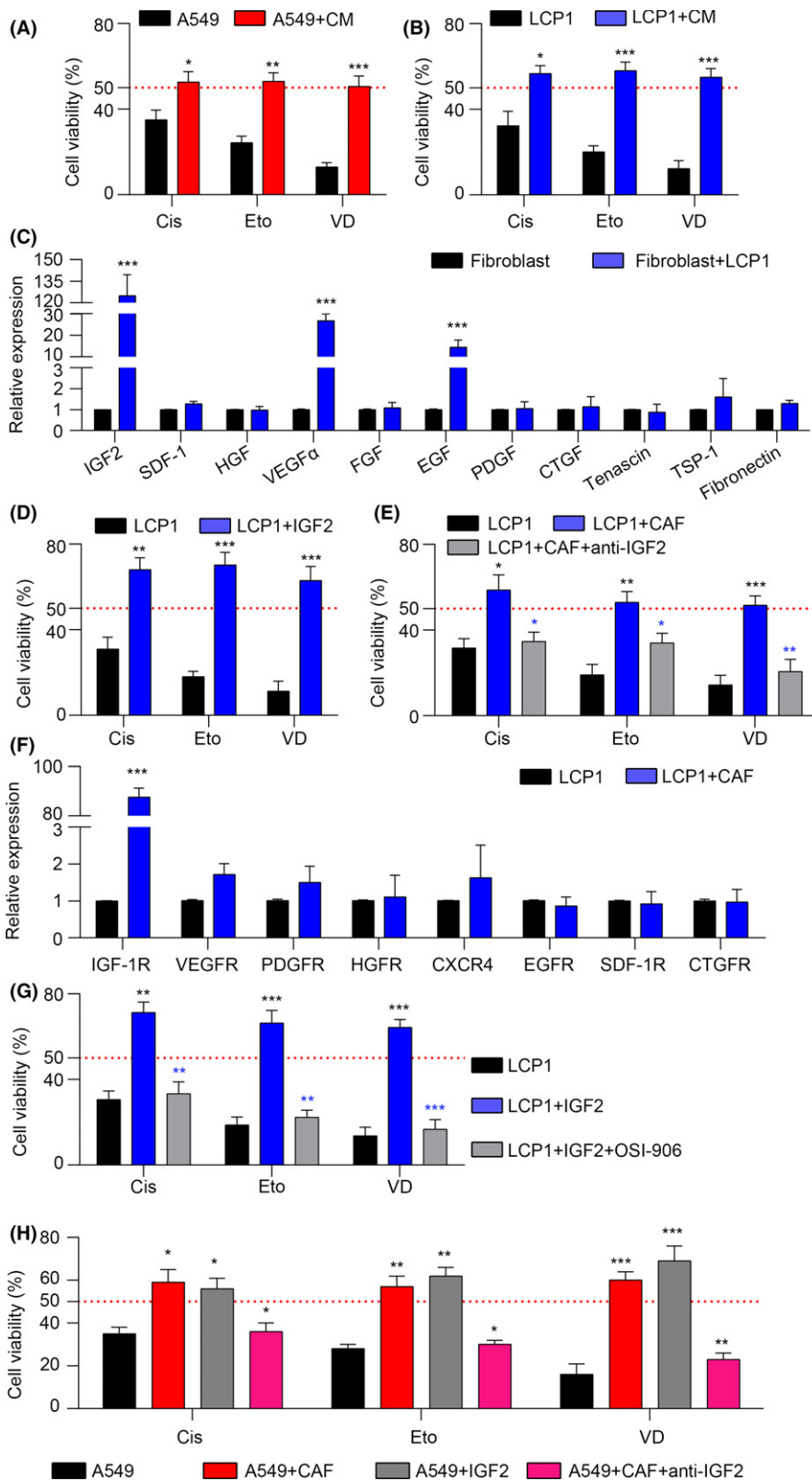


**FIGURE 2** Cancer-associated fibroblasts (CAF) induce the acquired chemo-resistance through an insulin-like growth factor 2 (IGF2)/insulin-like growth factor receptor-1 (IGF-1R) paracrine pathway. A, MTT assay of A549 cells treated with 400 nmol/L cisplatin (Cis), 150 μmol/L etoposide (Eto) and 800 nmol/L vinorelbine ditartrate (VD), respectively, with or without CAF medium (CM) pretreated (n = 3). B, MTT assay of LCP1 cells treated with Cis, Eto and VD, respectively, with or without CAF medium (CM) pretreated (n = 3). C, mRNA expression of IGF2, SDF-1, HGF, VEGFα, FGF, EGF, PDGF, CTGF, tenascin, TSP-1 and fibronectin in CAF cells co-culturing with or without LCP1 cells (n = 3). D, MTT assay of LCP1 cells treated with Cis, Eto and VD, respectively, with or without IGF2 pretreated (n = 3). E, MTT assay of LCP1 cells treated with Cis, Eto and VD, respectively, with or without CAF pre-co-cultured in the presence or absence of anti-IGF2 (n = 3). F, mRNA expression of IGF-1R, VEGFR, PDGFR, HGFR, CXCR4, EGFR, SDF-1R and CTGFR in LCP1 cells with or without CAF co-cultured (n = 3). G, MTT assay of LCP1 cells treated by Cis, Eto and VD, respectively, with or without IGF2 pretreated in the presence or absence of OSI-906 (n = 3). H, A549 cells were isolated from A549-bearing nude mice with CAF, IGF2, CAF and anti-IGF2 treatment for 1 wk; the cell viability was analyzed in the addition of Cis, Eto or VD by MTT assay (n = 3). The data are presented as the means ± SEM from 3 independent experiments. \**P* < .05; \*\**P* < .01; \*\*\**P* < .001; ns, not statistically significant

factors in the medium to promote NSCLC cell survival under stress of chemotherapy drugs. To further determine the key factors in the CAF-secreted cytokines involved in NSCLC drug resistance, we screened the expression of IGF2,<sup>21</sup> SDF-1,<sup>22</sup> HGF,<sup>23</sup> VEGFα,<sup>24</sup> FGF,<sup>25</sup>

EGF,<sup>26</sup> PDGF,<sup>27</sup> CTGF,<sup>28</sup> Tenascin,<sup>29</sup> TSP-1<sup>30</sup> and Fibronectin<sup>31</sup> in the CAF pre-co-cultured with or without LCP1 cells and found that IGF2, VEGFα and EGF were significantly upregulated, especially the IGF2 (Figure 2C). Moreover, we used the recombinant IGF2 to pre-

treat LCP1 and A549 cells, followed by cisplatin, etoposide and vinorelbine dihydrate treatment. We found that IGF2 could elevate the cell viability (Figures 2D and S2A). It was further demonstrated in the fibroblast and tumor cell co-culturing system that the cell viability was decreased with the application of anti-IGF2 antibody (Figures 2E and S2B). Consistently, we found that the expression of IGF2 in chemo-resistant samples was significantly higher than in chemo-sensitive samples, as evidenced by immunohistochemistry staining (Figure S2C). The above data indicated that IGF2, indeed, could induce the drug resistance in NSCLC cells. Numerous reports have shown that cytokines function through binding their corresponding receptors.<sup>32,33</sup> Thus, we screened for the expression of *IGF-1R*, *VEGFR*, *PDGFR*, *HGFR*, *CXCR4*, *EGFR*, *SDF-1R* and *CTGFR* in LCP1 cells pre-co-cultured with or without CAF. Consistent with the ligand expression, *IGF-1R* was highly expressed in LCP1 cells with CAF co-culturing (Figure 2F). Furthermore, we used OSI-906, the inhibitor of *IGF-1R*, to treat the IGF2-pretreated LCP1 and A549 cells, and found that the IGF2 induced LCP1 and that A549 drug resistance was blocked (Figures 2G and S2D). This indicates that drug resistance in NSCLC cells induced by IGF2 is *IGF-1R*-dependent. In addition, we addressed the effects of chemotherapy on CAF and/or LCP1 cells. We found that cisplatin, etoposide and vinorelbine dihydrate increased the secretion of IGF2 by CAF only in the presence of LCP1 cells and upregulated *IGF-1R* in LCP1 cells only with CAF that were co-cultured (Figure S2E,F). To further demonstrate that the IGF2 was secreted by CAF and examine the effects of CAF and IGF2 in NSCLC drug resistance, we isolated tumor cells from A549-bearing nude mice treated with CAF, IGF2 and CAF combined with IGF2 neutralizing antibody treatment and analyzed the cytotoxicity of chemotherapeutic drugs *ex vivo*. Consistent with the above data, CAF or IGF2 could effectively enhance the cell viability of A549 cells *in vivo*, while the blockade of IGF2 could reverse the drug resistance induced by CAF (Figure 2H). We conclude that CAF could mediate the drug resistance of NSCLC cells through the IGF2/*IGF-1R* paracrine pathway.

### 3.3 | The insulin-like growth factor 2/insulin-like growth factor receptor-1 signal triggers the AKT/Sox2 pathway to induce the acquired chemo-resistance

As a classic downstream molecule of the insulin-like growth factor (IGF) signaling axis, AKT is involved in cell survival, cell cycle, metabolism and drug resistance.<sup>34,35</sup> In addition, many studies have reported that AKT is correlated to drug resistance in hepatocellular carcinoma and prostate cancer models;<sup>36,37</sup> therefore, we evaluated the phosphorylation of AKT in A549 cells pre-co-cultured with CAF/recombinant IGF2 or not. We found that the expression of phospho-AKT was increased in the CAF/recombinant IGF2-treated A549 cells (Figure 3A), while adding anti-IGF2 significantly reduced the phospho-AKT level (Figure 3B). Furthermore, adding MK-2206<sup>38</sup> (an inhibitor for AKT) effectively reversed the

resistance of IGF2-treated A549 cells to the cisplatin, etoposide and vinorelbine dihydrate (Figure 3C). These results suggested that AKT may work as the downstream in the IGF2/*IGF-1R* axis in the acquisition of drug resistance in NSCLC cells.

It has been reported that Nanog, Oct4 and Sox2 are the main transcriptional factors in activating the AKT signaling pathway.<sup>39-41</sup> Thus, we analyzed the expression of *Nanog*, *Oct4* and *Sox2* in CAF-treated A549 and LCP1 cells, and we found that only the *Sox2* was significantly upregulated in both A549 and LCP1 NSCLC cells after co-culturing with CAF (Figure 3D,E). Correspondingly, the inducible expression of *Sox2* by CAF and/or recombinant IGF2 was verified using western blot (Figure 3F) and immunofluorescence (Figure 3G). The data indicated that CAF and/or IGF2 could induce the high expression of *Sox2* and its nuclear translocation. In addition, adding anti-IGF2 reversed the inducible expression of *Sox2* by CAF (Figure 3H). Furthermore, MK-2206 also markedly decreased the expression of *Sox2*, which was induced by IGF2 (Figure 3I). These data suggest that the inducible expression of *Sox2* may work as the downstream of IGF2/AKT pathway in the acquired drug resistance with CAF. Moreover, silencing of *Sox2* liberated IGF2 also resulted in the cisplatin, etoposide and vinorelbine dihydrate resistance (Figure 3J), which is in line with previous results. Taken together, we conclude that AKT/*Sox2* is involved in the IGF2/*IGF-1R*-induced drug resistance in NSCLC cells.

### 3.4 | Insulin-like growth factor 2 triggers the AKT/Sox2 pathway to elevate P glycoprotein expression

We have demonstrated that AKT/*Sox2* was involved in CAF inducing the acquired chemo-resistance, but we wondered how those signals participated in the NSCLC cells survival from chemotherapy. It has been reported that ATPase binding cassette (ABC) transporters mainly participate in drug efflux of cancer cells, leading to reduced cytotoxicity and drug resistance. Thus, we hypothesized that *Sox2* might play a role in ABC gene transcription. Using the JASPAR database, we predicted that *Sox2* had most putative binding sites in *ABCB1* promoter (Figure 4A). We also screen the expressions of ABC transporters, *ABCA2*, *ABCB1*, *ABCB4*, *ABCB11*, *ABCC1*, *ABCC2* and *ABCG2*, and found that the gene expression of *ABCB1*, which encodes P-GP, has the highest upregulation (nearly 274-fold) in A549 cells pre-co-cultured with CAF compared with control cells (Figure 4B). Moreover, the protein expression of P-GP was elevated in A549 cells with recombinant IGF2 treatment, and this upregulation was blocked when *Sox2* was silenced (Figure 4C). These data indicated that *Sox2* may mediate the P-GP expression in IGF2 induced the chemo-resistance of NSCLC cells. Furthermore, both CAF and recombinant IGF2 treatment elevated the expression of P-GP in A549 cells compared with control cells (Figure 4D), while adding anti-IGF2 or MK-2206 depressed the elevation (Figure 4E,F). These results indicate that P-GP participates in the drug-resistance process in NSCLC cells, which is induced by AKT/*Sox2* signal pathway.

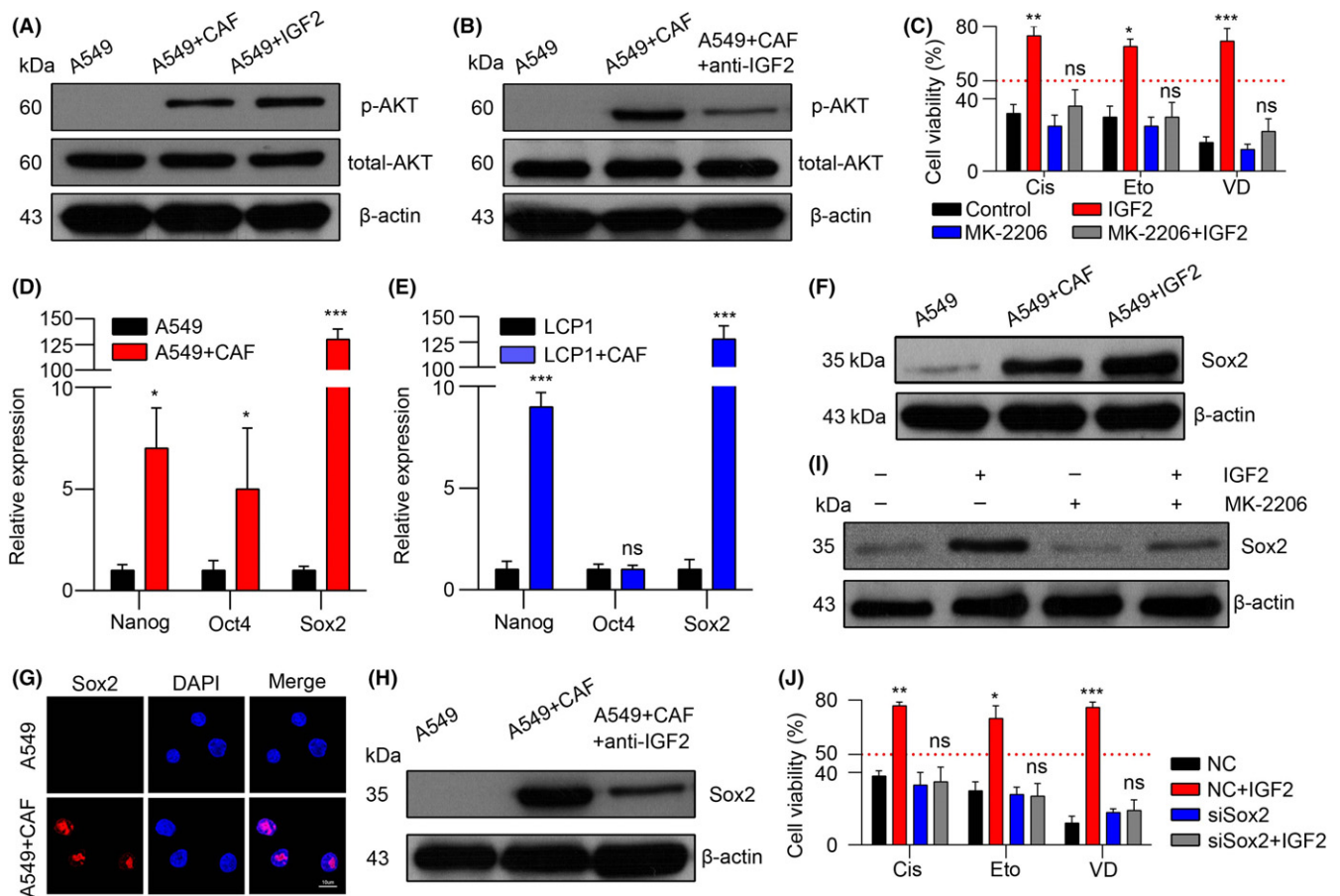


**FIGURE 3** The insulin-like growth factor 2 (IGF2)/insulin-like growth factor receptor-1 (IGF-1R) signal triggers the AKT/Sox2 pathway to induce the acquired chemo-resistance. A, Western blotting of p-AKT, total AKT and  $\beta$ -actin in A549 cells with or without CAF co-cultured or IGF2 treated. B, Western blotting of p-AKT, total AKT and  $\beta$ -actin in A549 cells with or without CAF co-cultured in the presence or absence of anti-IGF2. C, The MTT assay of A549 cells treated with Cis, Eto and VD with or without IGF2 pretreated in the presence or absence of MK-2206 ( $n = 3$ ). D, The mRNA expression of Nanog, Oct4 and Sox2 in A549 cells with or without CAF co-cultured ( $n = 3$ ). E, mRNA expression of Nanog, Oct4 and Sox2 in LCP1 cells with or without CAF co-cultured ( $n = 3$ ). F, Western blotting of Sox2 and  $\beta$ -actin in A549 cells with or without CAF co-cultured or IGF2 treated. G, Immunofluorescence of Sox2 in A549 cells with or without CAF co-cultured. Red, Sox2; blue, DAPI; scale bar, 10  $\mu$ m. H, Western blotting of Sox2 and  $\beta$ -actin in A549 cells with or without CAF co-cultured in the presence and absence of anti-IGF2. I, Western blotting of Sox2 and  $\beta$ -actin in A549 cells with or without IGF2 treated in the presence or absence of MK-2206. J, MTT assay in negative control (NC) or siSox2-transfected A549 cells treated with Cis, Eto and VD with or without IGF2 pretreated ( $n = 3$ ). The data was presented as the means  $\pm$  SEM from 3 independent experiments. \* $P < .05$ ; \*\* $P < .01$ ; \*\*\* $P < .001$ ; ns, not statistically significant

### 3.5 | Cancer-associated fibroblasts regulate chemo-resistance through P-GP to decrease drug retention and increase drug efflux

Because we have found that P-GP was upregulated in CAF and induced NSCLC chemo-resistance, we questioned the function of P-GP in this process. Strong evidence has been reported that P-GP may contribute to drug resistance in cancer by reducing drug uptake and enhancing drug efflux.<sup>5,42</sup> To investigate whether accumulated CAF-induced chemo-resistance in NSCLC tissue was associated with the drug accumulation, doxorubicin was employed for its strong fluorescence in the assessment of intracellular drug content by immunofluorescence or flow cytometry. Our data showed that pre-culturing with CAF decreased the doxorubicin retention in the

nucleus of A549 cells (Figure 5A) compared with monoculture. Correspondingly, we found that monoculture A549 cells absorbed doxorubicin in a time-dependent manner, while cells pre-co-cultured with CAF had less absorption over time (Figure 5B). In line with the data, we observed that the drug efflux in A549 cells pre-co-cultured with CAF was higher than control A549 cells at every time point (Figure 5C). These results indicated that CAF may decrease drug retention and increase drug efflux, leading to the anti-doxorubicin ability of A549 cells. Our previous data showed that adding recombinant IGF2 remarkably enhanced the chemo-resistance of A549 cells. To further verify, we pre-treated A549 cells with recombinant IGF2, followed by doxorubicin treatment. And we found that rhIGF2 pre-treatment reduced doxorubicin aggregation in the nucleus of A549 cells. However, adding OSI-906, an IGF-1R inhibitor, reversed the

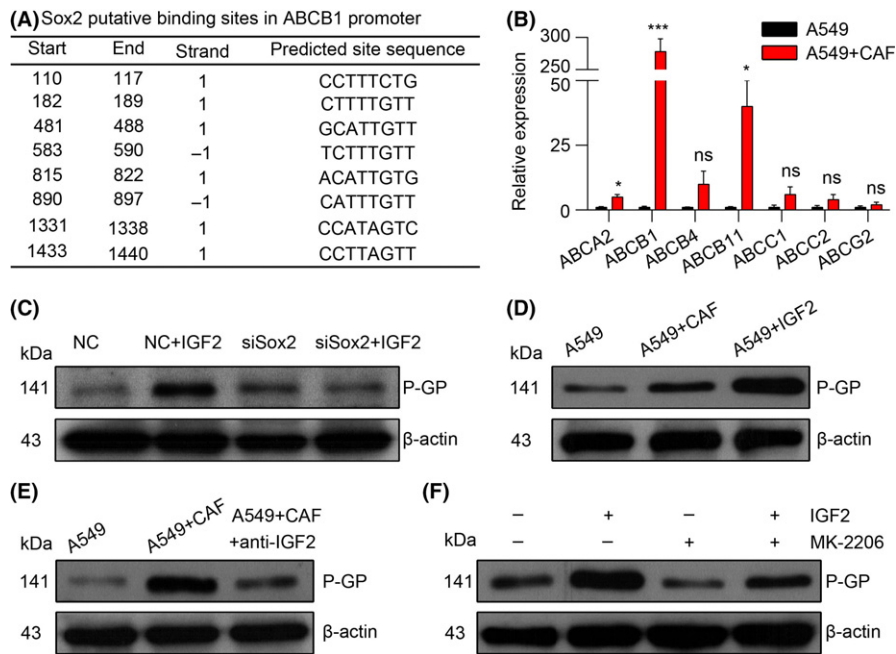


**FIGURE 4** Insulin-like growth factor 2 (IGF2) triggers the AKT/Sox2 pathway to elevate P-GP expression. A, Sox2 putative binding sites in ABCB1 promoter were acquired from the JASPAR database. B, mRNA expression of ABCA2, ABCB1, ABCB4, ABCB11, ABCC1, ABCC2 and ABCG2 in A549 cells with or without CAF co-cultured ( $n = 3$ ). C, Western blotting of P-GP and  $\beta$ -actin in negative control (NC) or siSox2 transfected A549 cells with or without IGF2 treated. D, Western blotting of P-GP and  $\beta$ -actin in A549 cells with or without CAF co-cultured or IGF2 treated. E, Western blotting of P-GP and  $\beta$ -actin in A549 cells with or without CAF co-cultured in the presence or absence of anti-IGF2. F, Western blotting of P-GP and  $\beta$ -actin in A549 cells with or without IGF2 treated in the presence or absence of MK-2206. The data are presented as the means  $\pm$  SEM from 3 independent experiments. \* $P < .05$ ; \*\* $P < .01$ ; \*\*\* $P < .001$ ; ns, not statistically significant

doxorubicin accumulation (Figure 5D). Similarly, we found that the doxorubicin absorption was damped but the efflux was increased in A549 cells in a time-dependent manner with IGF2 pretreatment, and the addition of IGF-1R inhibitor reversed the doxorubicin distribution (Figure 5E,F). Next, to further verify whether P-GP was involved in the drug efflux, we used verapamil, an inhibitor of P-GP, to treat A549 cells pre-co-cultured with CAF, and followed with doxorubicin treatment; we found that the doxorubicin retention in the nucleus was recorded again (Figure 5G). Furthermore, the cell death rate was significantly elevated in CAF co-cultured A549 cells when verapamil was added (Figure 5H). Taken together, we conclude that CAF induced chemo-resistance by P-GP to decrease drug retention and increase drug efflux.

### 3.6 | Blockade insulin-like growth factor 2/insulin-like growth factor receptor-1 signal relieves chemotherapy drug resistance in non-small cell lung cancer in vivo

To evaluate the CAF-induced drug resistance in vivo, we generated a xenograft mouse model using A549 cells injected subcutaneously and treated with OSI-906, cisplatin, etoposide or vinorelbine ditartrate. Tumor volume data showed that single OSI-906 or cisplatin treatment slightly inhibited tumor growth, while the combination significantly reduced the tumor volume compared with the PBS

treatment (Figure 6A upper). In line with the data, injections with single OSI-906 or cisplatin failed to prolong the survival time of tumor-bearing mice, while combining treatment significantly extended the life of mice (Figure 6A, bottom), indicating that blocking IGF2/IGF-1R signals effectively reduced the drug resistance in NSCLC. Similar results were achieved when employing etoposide and vinorelbine ditartrate (Figure 6B,C). Overall, these results suggest the therapeutic potential of combining chemotherapy drugs with IGF2/IGF-1R inhibitors in NSCLC treatment.

## 4 | DISCUSSION

In our study, we found the CAF plays a crucial role in the development and maintenance of NSCLC cells' multi-drug resistance. These CAF isolated from tumor tissues with high chemotherapy resistance facilitate NSCLC cell drug resistance. The cancer cells would not be able to maintain the phenotype without the help of CAF feeders. Previous research revealed that CAF could participate in different stages of tumor progression, including EMT,<sup>43,44</sup> tumor stemness maintenance<sup>45</sup> and metastasis,<sup>6</sup> through secretion of several cytokines or components that activated important signaling pathways. Our studies indicate that CAF regulate the NSCLC cell drug resistance in a paracrine manner through secretion of IGF2 and the activation of AKT/Sox2/P-GP signals in cancer cells. The IGF2 produced by CAF



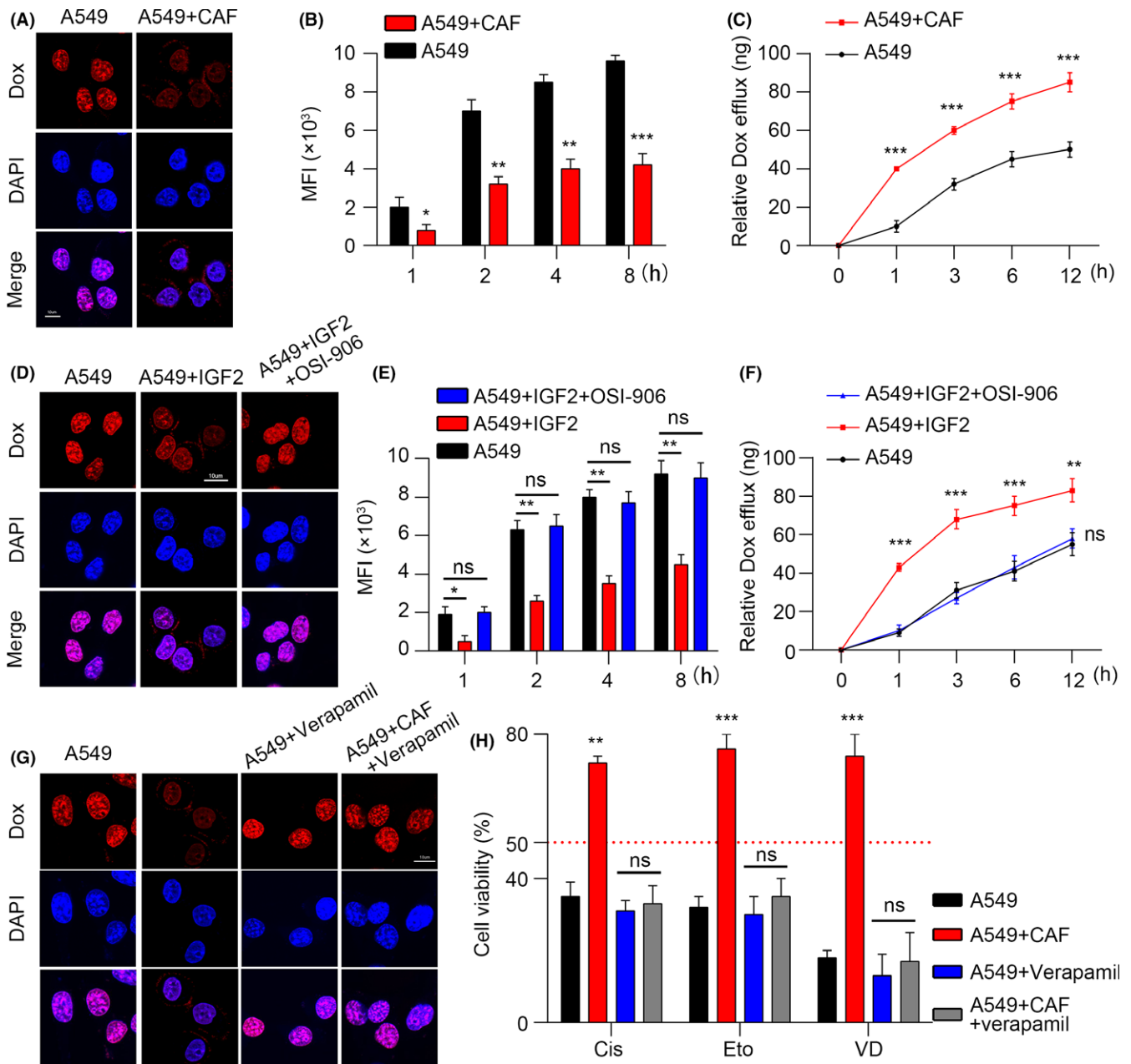


**FIGURE 5** Cancer-associated fibroblasts (CAF) regulate chemo-resistance through P-GP to decrease drug retention and increase drug efflux. A, The fluorescence of doxorubicin (Dox) in A549 cells with or without CAF pre-co-cultured. Red, Dox; blue, DAPI; scale bar, 10  $\mu\text{m}$ . B, Mean fluorescence intensity (MFI) of Dox in A549 cells with or without CAF pre-co-cultured at different time points ( $n = 4$ ). C, Released Dox in the supernatants of A549 cells with or without CAF pre-co-cultured at different time points ( $n = 3$ ). D, Fluorescence of Dox in A549 cells with or without IGF2 pretreated in the presence or absence of OSI-906. Red, Dox; blue, DAPI; scale bar, 10  $\mu\text{m}$ . E, MFI of Dox in A549 cells with or without IGF2 pretreated in the presence or absence of OSI-906 at different time points ( $n = 3$ ). F, Released Dox in the supernatants of A549 cells with or without IGF2 pretreated in the presence or absence of OSI-906 at different time points ( $n = 3$ ). G, Fluorescence of Dox in A549 cells with or without CAF pre-co-cultured in the presence or absence of verapamil. H, MTT assay of A549 cells treated with Cis, Eto and VD with or without CAF pre-co-cultured in the presence or absence of verapamil ( $n = 3$ ). The data are presented as the means  $\pm$  SEM from 3 independent experiments. \* $P < .05$ ; \*\* $P < .01$ ; \*\*\* $P < .001$ ; ns, not statistically significant

activates the AKT pathways by binding to the membrane receptor IGF-1R in NSCLC cells to activate AKT. Then the phosphorylated AKT triggers transcription factor Sox2 nucleus translocation to bind the promoter region of the ABCB1 gene. Finally, the P-GP expression is upregulated, resulting in the development of drug resistance (Figure 6D).

Various crucial features are believed to result in the development of multi-drug resistance, including ATP-binding cassette (ABC) transporter protein overexpression, upregulation of anti-apoptotic proteins such as BCL-XL and BCL-2, enhanced DNA damage repair and cytokines in the tumor microenvironment.<sup>5</sup> It was demonstrated that the tumor microenvironment plays a crucial role in tumor

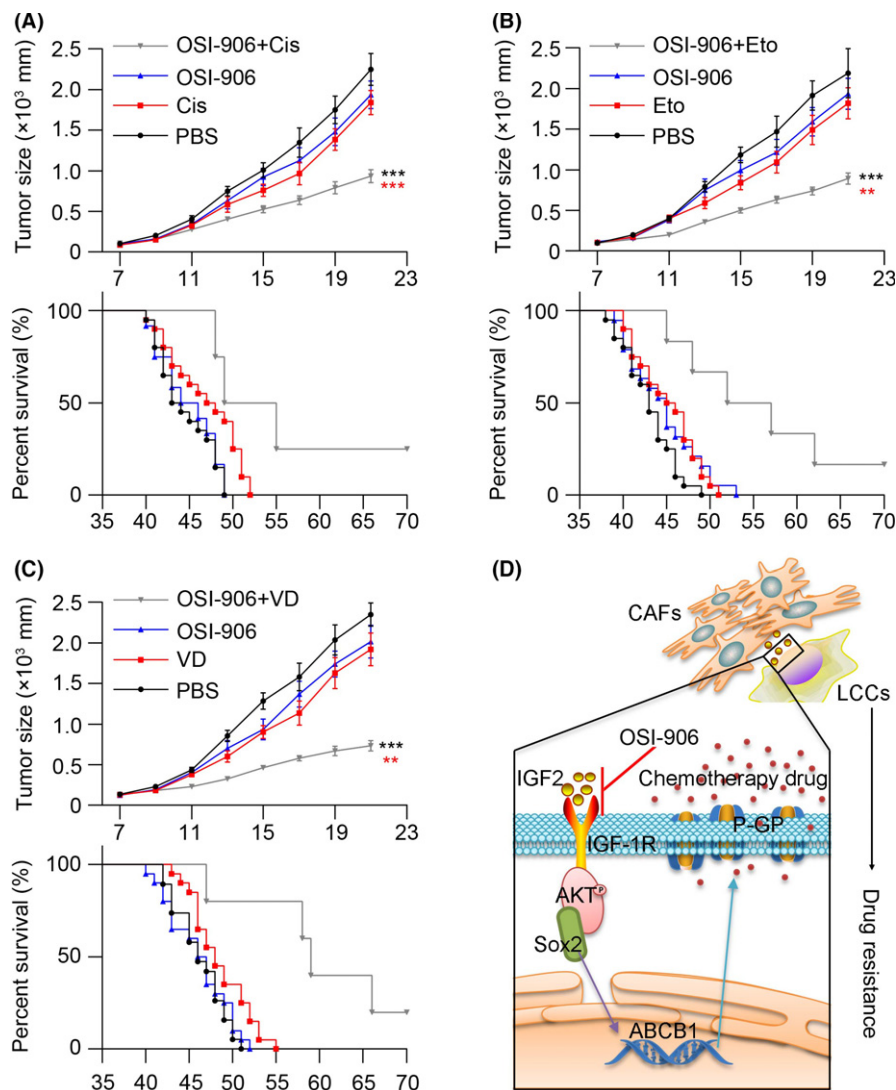


**FIGURE 6** Blockade insulin-like growth factor 2 (IGF2)/insulin-like growth factor receptor-1 (IGF-1R) signal relieves chemotherapy drug resistance in lung cancer. A, Mean tumor volume of subcutaneous A549 implants in PBS, Cis, OSI-906 or Cis combining OSI-906-treated nod-scid mice (top,  $n = 6$ ); the long-term survival of tumor-bearing mice treated with PBS, Cis, OSI-906 or Cis combining OSI-906 (bottom,  $n = 20$ ). B, Mean tumor volume of subcutaneous A549 implants in PBS, Eto, OSI-906 or Eto combining OSI-906-treated nod-scid mice (top,  $n = 6$ ); the long-term survival of tumor bearing mice treated with PBS, Eto, OSI-906 or Eto combining OSI-906 (bottom,  $n = 20$ ). C, Mean tumor volume of subcutaneous A549 implants in PBS, VD, OSI-906 or VD combining OSI-906 treated nod-scid mice (top,  $n = 6$ ); the long-term survival of tumor-bearing mice treated with PBS, VD, OSI-906 or VD combining OSI-906 (bottom,  $n = 20$ ). D, Cancer-associated fibroblasts (CAF) produce IGF2 to bind IGF-1R in lung cancer cells (LCC) and activate the AKT/Sox2 pathways. Along with the Sox2 nucleus translocation, the transcription of ABCB1 gene is enhanced and the expression of P-GP is evaluated to pump out the chemotherapy drug. Using OSI-906 to block IGF2/IGF-1R signal and combining with chemotherapy drug could reverse the drug resistance of lung cancer cells. The data was presented as the means  $\pm$  SEM from 3 independent experiments. \* $P < .05$ ; \*\* $P < .01$ ; \*\*\* $P < .001$ ; ns, not statistically significant

progression,<sup>6,46</sup> which tumor cells depend on for sustained growth, metastasis and invasion. Furthermore, several studies have demonstrated that the microenvironment is capable of regulating cancer cell stemness or drug resistance through signaling pathway activation.<sup>47,48</sup> However, traditional cancer treatments focus on inhibiting tumor cell growth but ignoring the tumor microenvironment elements.<sup>49-51</sup> Many studies have attempted to reverse drug resistance through various strategies, including the combination of 2 or more anticancer therapeutic agents,<sup>52,53</sup> inhibitors of ABC transporters,<sup>54,55</sup> or application of chemosensitizers,<sup>56</sup> which has been

proven to be able to reverse drug resistance and inhibit tumor growth in the early stages. However, recent research revealed that the tumor microenvironment could induce drug resistance development of normal cancer cells and tumor tissues could reacquire the drug resistance under the appropriate microenvironment after chemotherapy.<sup>55,57</sup> Thus, solely directly targeting cancer cells may not be sufficient to reverse the cancer drug resistance; instead, blocking the interaction between CAF and cancer cells could serve as the basis of an innovative treatment to reverse the cancer drug resistance.

It was reported that CAF in lung cancer microenvironment are associated with cancer stemness maintenance, cell proliferation and cancer metastasis.<sup>12,58,59</sup> However, the specific relationship between CAF and cancer cell behavior remains unclear. In our study, we further examined the precipitating factors of chemotherapy failure in NSCLC patients, and found that a mass of CAF in tumor tissues would induce the development of cancer cell drug resistance via an IGF2/IGF-1R paracrine pathway. Hence, OSI-906, an inhibitor of IGF-1R, could serve as a potential agent to block the IGF2/IGF-1R paracrine pathway induced by CAF and be combined with multiple chemotherapeutic agents to effectively reverse the drug resistance and inhibit NSCLC progression.

In summary, our data described a novel role of CAF in resistance to multiple chemotherapeutic drugs in NSCLC. In addition, CAF regulate the drug resistance in a paracrine manner through the IGF2/IGF-1R/Sox2/P-GP pathway. The combination of a selective small-molecule inhibitor to IGF-1R with chemotherapeutic agents will be explored as a potential therapeutic strategy for anticancer therapy.

## ACKNOWLEDGMENTS

This study was supported by the Research and Development of Bio-compatible Airway Stent (No. 2015AA020301).

## CONFLICT OF INTEREST

The authors have no conflicts of interest to declare.

## ORCID

Quanhui Zhang  <http://orcid.org/0000-0003-1358-3500>

## REFERENCES

- Siegel RL, Miller KD, Jemal A. Cancer statistics, 2016. *CA Cancer J Clin*. 2016;66:7-30.
- Sheng B, Qi C, Liu B, Lin Y, Fu T, Zeng Q. Increased HSP27 correlates with malignant biological behavior of non-small cell lung cancer and predicts patient's survival. *Sci Rep*. 2017;7:13807.
- Sequist LV, Bell DW, Lynch TJ, Haber DA. Molecular predictors of response to epidermal growth factor receptor antagonists in non-small-cell lung cancer. *J Clin Oncol*. 2007;25:587-595.
- Shih JY, Gow CH, Yang PC. EGFR mutation conferring primary resistance to gefitinib in non-small-cell lung cancer. *N Engl J Med*. 2005;353:207-208.
- Holohan C, Van Schaeybroeck S, Longley DB, Johnston PG. Cancer drug resistance: an evolving paradigm. *Nat Rev Cancer*. 2013;13:714-726.
- Quail DF, Joyce JA. Microenvironmental regulation of tumor progression and metastasis. *Nat Med*. 2013;19:1423-1437.
- Pistore C, Giannoni E, Colangelo T, et al. DNA methylation variations are required for epithelial-to-mesenchymal transition induced by cancer-associated fibroblasts in prostate cancer cells. *Oncogene*. 2017;5:159.
- Turner N, Grose R. Fibroblast growth factor signalling: from development to cancer. *Nat Rev Cancer*. 2010;10:116-129.
- Zhai Y, Chai L, Chen J. The relationship between the expressions of tumor associated fibroblasts Cav-1 and MCT4 and the prognosis of papillary carcinoma of breast. *Pak J Pharm Sci*. 2017;30:263-272.
- Allaoui R, Bergenfelz C, Mohlin S, et al. Cancer-associated fibroblast-secreted CXCL16 attracts monocytes to promote stroma activation in triple-negative breast cancers. *Nat Commun*. 2016;7:13050.
- Hassona Y, Cirillo N, Heesom K, Parkinson EK, Prime SS. Senescent cancer-associated fibroblasts secrete active MMP-2 that promotes keratinocyte dis-cohesion and invasion. *Br J Cancer*. 2014;111:1230-1237.
- Kalluri R. The biology and function of fibroblasts in cancer. *Nat Rev Cancer*. 2016;16:582-598.
- Alderton GK. Therapeutic resistance: fibroblasts restrain drug sensitivity. *Nat Rev Cancer*. 2015;15:318-319.
- Zhong S, Teo WE, Zhu X, Beuerman RW, Ramakrishna S, Yung LY. An aligned nanofibrous collagen scaffold by electrospinning and its effects on in vitro fibroblast culture. *J Biomed Mater Res A*. 2006;79:456-463.
- Matsuwaki R, Ishii G, Zenke Y, et al. Immunophenotypic features of metastatic lymph node tumors to predict recurrence in N2 lung squamous cell carcinoma. *Cancer Sci*. 2014;105:905-911.
- Mao Y, Wang X, Zheng F, et al. The tumor-inhibitory effectiveness of a novel anti-Trop2 Fab conjugate in pancreatic cancer. *Oncotarget*. 2016;7:24810-24823.
- Orimo A, Gupta PB, Sgroi DC, et al. Stromal fibroblasts present in invasive human breast carcinomas promote tumor growth and angiogenesis through elevated SDF-1/CXCL12 secretion. *Cell*. 2005;121:335-348.
- Saeki T, Tsuruo T, Sato W, Nishikawa K. Drug resistance in chemotherapy for breast cancer. *Cancer Chemother Pharmacol*. 2005;1:84-89.
- Leonessa F, Clarke R. ATP binding cassette transporters and drug resistance in breast cancer. *Endocr Relat Cancer*. 2003;10:43-73.
- Mimeault M, Hauke R, Batra SK. Recent advances on the molecular mechanisms involved in the drug resistance of cancer cells and novel targeting therapies. *Clin Pharmacol Ther*. 2008;83:673-691.
- Ostman A, Augsten M. Cancer-associated fibroblasts and tumor growth—bystanders turning into key players. *Curr Opin Genet Dev*. 2009;19:67-73.
- Feig C, Jones JO, Kraman M, et al. Targeting CXCL12 from FAP-expressing carcinoma-associated fibroblasts synergizes with anti-PD-L1 immunotherapy in pancreatic cancer. *Proc Natl Acad Sci U S A*. 2013;110:20212-20217.
- Kikuchi K, McNamara KM, Miki Y, et al. Effects of cytokines derived from cancer-associated fibroblasts on androgen synthetic enzymes in estrogen receptor-negative breast carcinoma. *Breast Cancer Res Treat*. 2017;166:709-723.
- Pula B, Wojnar A, Witkiewicz W, Dziegiel P, Podhorska-Okolow M. Podoplanin expression in cancer-associated fibroblasts correlates with VEGF-C expression in cancer cells of invasive ductal breast carcinoma. *Neoplasma*. 2013;60:516-524.
- Sun Y, Fan X, Zhang Q, Shi X, Xu G, Zou C. Cancer-associated fibroblasts secrete FGF-1 to promote ovarian proliferation, migration, and invasion through the activation of FGF-1/FGFR4 signaling. *Tumour Biol*. 2017;39:1010428317712592.
- Chu TY, Yang JT, Huang TH, Liu HW. Crosstalk with cancer-associated fibroblasts increases the growth and radiation survival of cervical cancer cells. *Radiat Res*. 2014;181:540-547.
- Nwani NG, Deguiz ML, Jimenez B, et al. Melanoma cells block PEDF Production in fibroblasts to induce the tumor-promoting phenotype of cancer-associated fibroblasts. *Cancer Res*. 2016;76:2265-2276.
- Capparelli C, Whitaker-Menezes D, Guido C, et al. CTGF drives autophagy, glycolysis and senescence in cancer-associated fibroblasts via HIF1 activation, metabolically promoting tumor growth. *Cell Cycle*. 2012;11:2272-2284.

29. Yang Z, Ni W, Cui C, Fang L, Xuan Y. Tenascin C is a prognostic determinant and potential cancer-associated fibroblasts marker for breast ductal carcinoma. *Exp Mol Pathol.* 2017;102:262-267.
30. Spaeth EL, Dembinski JL, Sasser AK, et al. Mesenchymal stem cell transition to tumor-associated fibroblasts contributes to fibrovascular network expansion and tumor progression. *PLoS ONE.* 2009;4:7.
31. Attieh Y, Clark AG, Grass C, et al. Cancer-associated fibroblasts lead tumor invasion through integrin-beta3-dependent fibronectin assembly. *J Cell Biol.* 2017;216:3509-3520.
32. Schmitt RM, Bruyns E, Snodgrass HR. Hematopoietic development of embryonic stem cells in vitro: cytokine and receptor gene expression. *Genes Dev.* 1991;5:728-740.
33. Ware CF, VanArsdale S, VanArsdale TL. Apoptosis mediated by the TNF-related cytokine and receptor families. *J Cell Biochem.* 1996;60:47-55.
34. Testa JR, Tsichlis PN. AKT signaling in normal and malignant cells. *Oncogene.* 2005;24:7391-7393.
35. Denduluri SK, Idowu O, Wang Z, et al. Insulin-like growth factor (IGF) signaling in tumorigenesis and the development of cancer drug resistance. *Genes Dis.* 2015;2:13-25.
36. Wang Q, Yu WN, Chen X, et al. Spontaneous hepatocellular carcinoma after the combined deletion of Akt isoforms. *Cancer Cell.* 2016;29:523-535.
37. Domingo-Domenech J, Vidal SJ, Rodriguez-Bravo V, et al. Suppression of acquired docetaxel resistance in prostate cancer through depletion of notch- and hedgehog-dependent tumor-initiating cells. *Cancer Cell.* 2012;22:373-388.
38. Yap TA, Yan L, Patnaik A, et al. First-in-man clinical trial of the oral pan-AKT inhibitor MK-2206 in patients with advanced solid tumors. *J Clin Oncol.* 2011;29:4688-4695.
39. Liu CW, Li CH, Peng YJ, et al. Snail regulates Nanog status during the epithelial-mesenchymal transition via the Smad1/Akt/GSK3beta signaling pathway in non-small-cell lung cancer. *Oncotarget.* 2014;5:3880-3894.
40. Wang XQ, Ongkeko WM, Chen L, et al. Octamer 4 (Oct4) mediates chemotherapeutic drug resistance in liver cancer cells through a potential Oct4-AKT-ATP-binding cassette G2 pathway. *Hepatology.* 2010;52:528-539.
41. Singh S, Trevino J, Bora-Singhal N, et al. EGFR/Src/Akt signaling modulates Sox2 expression and self-renewal of stem-like side-population cells in non-small cell lung cancer. *Mol Cancer.* 2012;11:1476-4598.
42. Zahreddine H, Borden KL. Mechanisms and insights into drug resistance in cancer. *Front Pharmacol.* 2013;4:28.
43. De Craene B, Bex G. Regulatory networks defining EMT during cancer initiation and progression. *Nat Rev Cancer.* 2013;13:97-110.
44. Seton-Rogers S. Epithelial-mesenchymal transition: untangling EMT's functions. *Nat Rev Cancer.* 2016;16:27.
45. Hsu YC, Li L, Fuchs E. Emerging interactions between skin stem cells and their niches. *Nat Med.* 2014;20:847-856.
46. Gajewski TF, Schreiber H, Fu YX. Innate and adaptive immune cells in the tumor microenvironment. *Nat Immunol.* 2013;14:1014-1022.
47. Nagarsheth N, Wicha MS, Zou W. Chemokines in the cancer microenvironment and their relevance in cancer immunotherapy. *Nat Rev Immunol.* 2017;30:49.
48. Medema JP. Cancer stem cells: the challenges ahead. *Nat Cell Biol.* 2013;15:338-344.
49. Seguin L, Kato S, Franovic A, et al. An integrin beta(3)-KRAS-Ra1B complex drives tumour stemness and resistance to EGFR inhibition. *Nat Cell Biol.* 2014;16:457-468.
50. Liu N, Liu C, Li X, et al. A novel proteasome inhibitor suppresses tumor growth via targeting both 19S proteasome deubiquitinases and 20S proteolytic peptidases. *Sci Rep.* 2014;4:5240.
51. Hirano S, Quach HT, Watanabe T, et al. Irciniastatin A, a pederin-type translation inhibitor, promotes ectodomain shedding of cell-surface tumor necrosis factor receptor 1. *J Antibiot.* 2015;68:417-420.
52. Mathijssen RH, Sparreboom A, Verweij J. Determining the optimal dose in the development of anticancer agents. *Nat Rev Clin Oncol.* 2014;11:272-281.
53. Espana-Serrano L, Chougule MB. Enhanced anticancer activity of PF-04691502, a dual PI3K/mTOR inhibitor, in combination with VEGF siRNA against non-small-cell lung cancer. *Mol Ther Nucleic Acids.* 2016;5:90.
54. Locher KP. Mechanistic diversity in ATP-binding cassette (ABC) transporters. *Nat Struct Mol Biol.* 2016;23:487-493.
55. Tarapcsak S, Szaloki G, Telbisz A, et al. Interactions of retinoids with the ABC transporters P-glycoprotein and breast cancer resistance protein. *Sci Rep.* 2017;7:41376.
56. D'Ambrogio A, Nagaoka K, Richter JD. Translational control of cell growth and malignancy by the CPEBs. *Nat Rev Cancer.* 2013;13:283-290.
57. McCarthy N. Drug resistance: making a point. *Nat Rev Cancer.* 2014;14:28.
58. Wagner EF. Cancer: fibroblasts for all seasons. *Nature.* 2016;530:42-43.
59. Martinez-Outschoorn UE, Sotgia F, Lisanti MP. Caveolae and signalling in cancer. *Nat Rev Cancer.* 2015;15:225-237.

## SUPPORTING INFORMATION

Additional Supporting Information may be found online in the supporting information tab for this article.

**How to cite this article:** Zhang Q, Yang J, Bai J, Ren J. Reverse of non-small cell lung cancer drug resistance induced by cancer-associated fibroblasts via a paracrine pathway. *Cancer Sci.* 2018;109:944-955. <https://doi.org/10.1111/cas.13520>